Assessment of PVS enhancement methods using a three-dimensional computational model: supplementary material

3 Results

For illustration purposes, we show precision-recall curves yielded by the Frangi, Jerman, and RORPO filters for 4-mm length and 2-mm width PVS in different conditions. We selected a PVS with such dimensions as it was found an average size in the study of reference (Ballerini et al., 2020).

3.2.1 Slice thickness
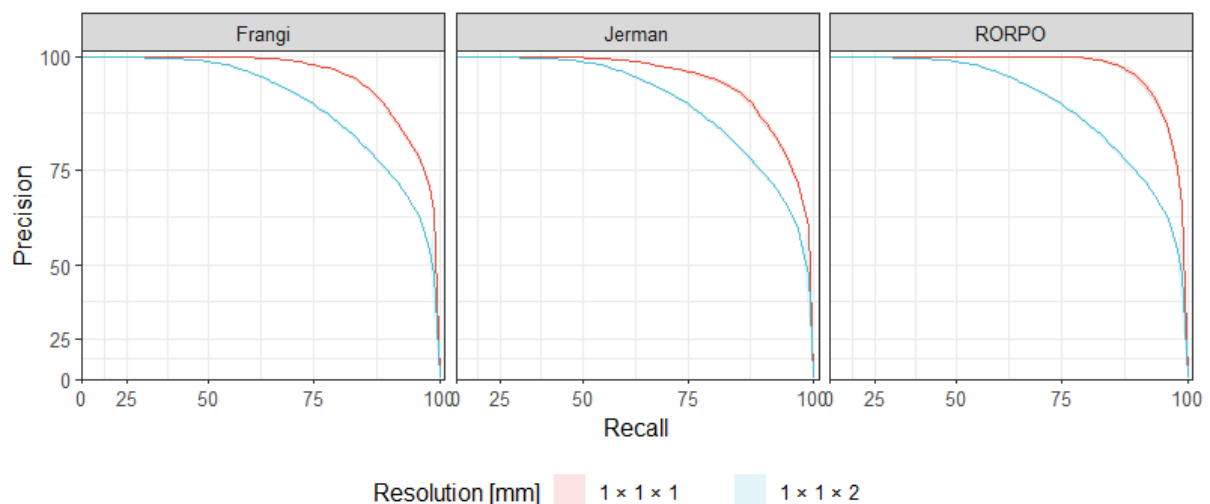
Figure S1. Precision-recall curve obtained by the Frangi, Jerman, and RORPO filters on a 4-mm length and 2-mm width PVS after sampling. Lines and shadowed areas represent mean precision-recall curves and their confidence interval, respectively.

3.2.2 Motion artefacts
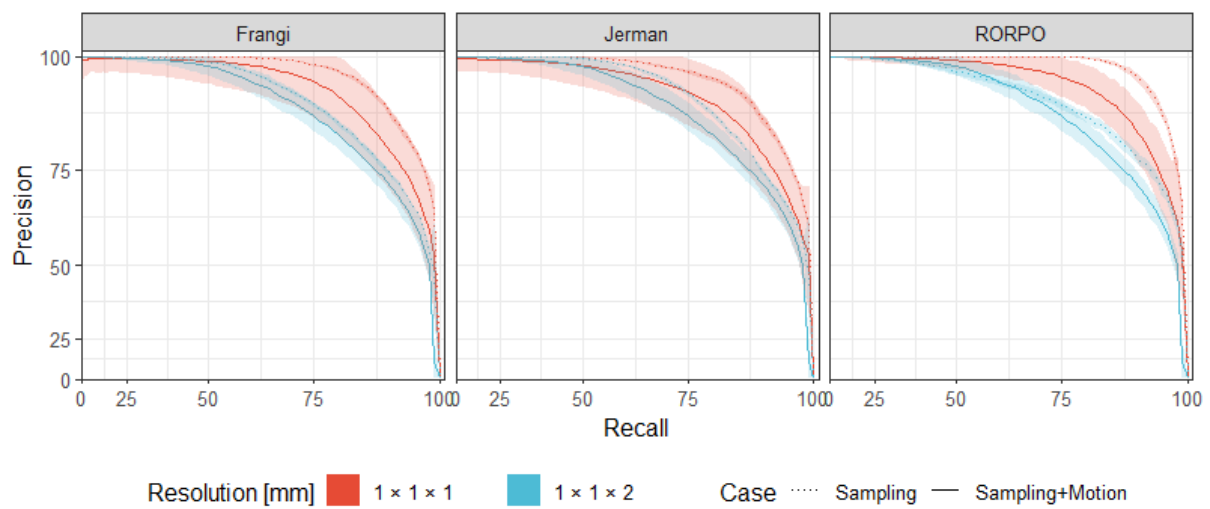
Figure S2. Precision-recall curve obtained by the Frangi, Jerman, and RORPO filters on a 4-mm length and 2-mm width PVS after sampling and incorporating motion artefacts. Lines and shadowed areas represent mean precision-recall curves and their confidence interval, respectively.

3.2.3 Rician noise
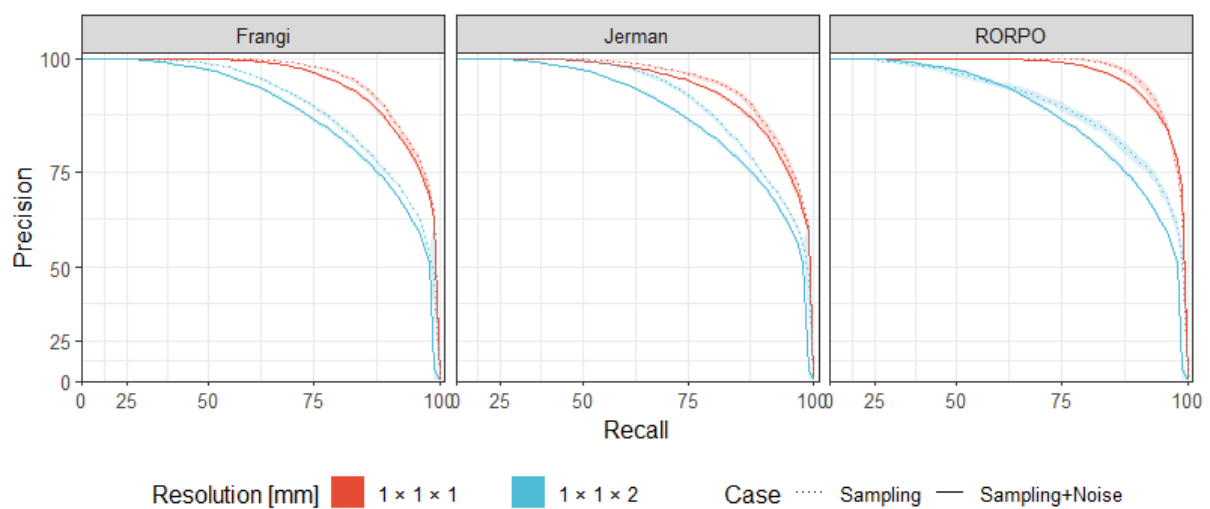
Figure S3. Precision-recall curve obtained by the Frangi, Jerman, and RORPO filters on a 4-mm length and 2-mm width PVS after sampling and adding Rician noise. Lines and shadowed areas represent mean precision-recall curves and their confidence interval, respectively.

3.3 Effect of pathological regions
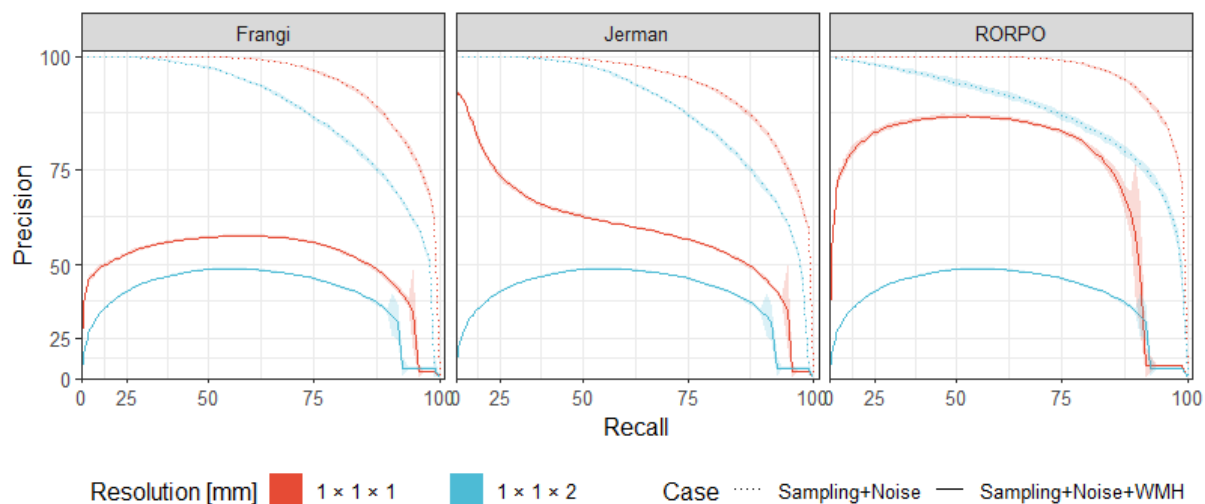
Figure S4. Precision-recall curve obtained by the Frangi, Jerman, and RORPO filters on a 4-mm length and 2-mm width PVS after sampling, noise, and WMH. Lines and shadowed areas represent mean precision-recall curves and their confidence interval, respectively.
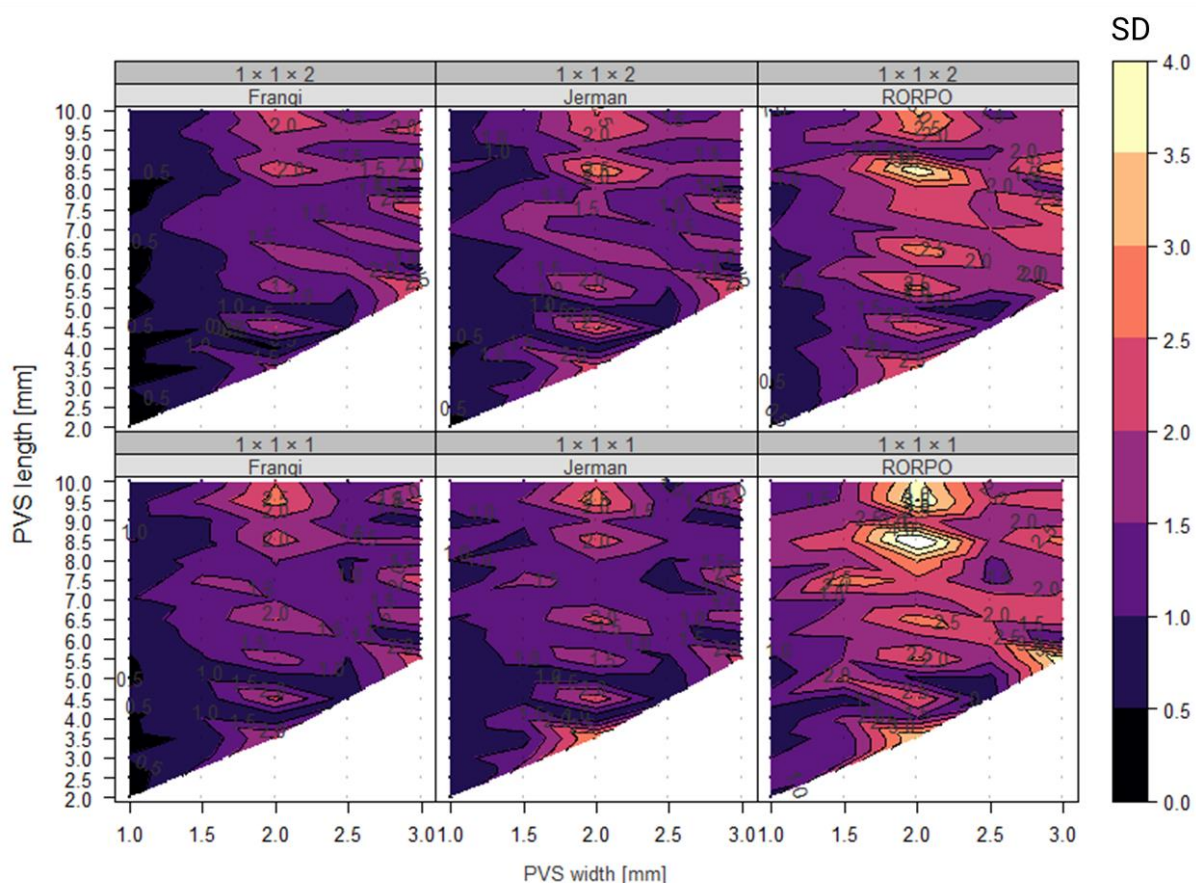
Figure S5. Effect of WMH in addition to sampling and Rician noise on the standard deviation of the area under precision-recall curve. We consider two scanning resolutions, 1 × 1 × 1 (bottom row) and 1 × 1 × 2 (top row) mm, to explore the impact of isotropic and anisotropic voxels on segmentation performance.

White regions represent cases that were not considered (width >= length, eccentricity < 0.8, or lack of PVS visibility). Imaging considerations: k-space sampling.

References

Ballerini, L., Booth, T., Valdés Hernández, M. del C., Wiseman, S., Lovreglio, R., Muñoz Maniega, S., … Wardlaw, J. (2020). Computational quantification of brain perivascular space morphologies: Associations with vascular risk factors and white matter hyperintensities. A study in the Lothian Birth Cohort 1936. *NeuroImage: Clinical*, *25*(November 2019), 102120. https://doi.org/10.1016/j.nicl.2019.102120